

## An Anion Radical Precursor in the Nucleophilic Substitution of *p*-Dinitrobenzene

Takehiro ABE and Yusaku IKEGAMI\*

College of General Education, Tohoku University, Kawauchi, Sendai 980

\* Chemical Research Institute of Non-Aqueous Solutions, Tohoku University, Katahira-2-chome, Sendai 980

(Received May 4, 1977)

Appearance of *p*-dinitrobenzene anion radical has been demonstrated by visible and ESR spectroscopy in the replacement of the one nitro group of *p*-dinitrobenzene by hydroxide ion in aqueous dimethyl sulfoxide. The formation of the anion radical seems to be due to the direct electron transfer from hydroxide ion to *p*-dinitrobenzene. The results of kinetic studies suggest that the anion radical is a precursor in the substitution reaction.

It has been strongly postulated that an *o*-dinitrobenzene anion radical is a precursor in the substitution reaction of the one nitro group of *o*-dinitrobenzene (*o*-DNB) by hydroxide ion in aqueous dimethyl sulfoxide (DMSO).<sup>1)</sup> The anion-radical precursor mechanism<sup>2)</sup> essentially differs from the widely-accepted conventional one, in which the nucleophilic aromatic substitution should proceed only *via* the Meisenheimer-type intermediate.

In order to pursue the anion-radical precursor mechanism, the following investigations have been made on a similar substitution reaction of *p*-dinitrobenzene (*p*-DNB).<sup>3)</sup> (1) Demonstration of the appearance of *p*-DNB<sup>•−</sup> (the *p*-dinitrobenzene anion radical) by visible and ESR spectroscopy. (2) Discussion on the possibility of the direct electron-transfer from the nucleophilic reagent to *p*-DNB. (3) Kinetic studies for confirmation of the view that the anion radical is the precursor in the replacement of the one nitro group of *p*-DNB by hydroxide ion in aqueous DMSO. Comparison of the results with those for *o*-DNB is made.

### Experimental

Commercial *p*-DNB was purified by recrystallization from benzene. DMSO was kept in contact with barium oxide for a week and fractionated twice under reduced pressure.

Unless otherwise stated, the mixing of degassed DMSO solutions of *p*-DNB with degassed DMSO solutions of sodium hydroxide was carried out in sealed cells for the measurements of electronic and ESR spectra. Before degassing, the cells in which the DMSO solutions had been placed were sealed by flame after blowing dry argon through the cells, since DMSO considerably takes up carbon dioxide. Unless argon is blown, the hydroxide ion in the DMSO solution placed in the cell is considerably consumed. Path lengths of 0.1–3 cm were available for the measurements of electronic spectra. Electronic-spectral changes were recorded with a Cary 14 recording spectrophotometer equipped with a thermostated cell compartment. ESR spectra were recorded with a Varian E-4 EPR spectrometer.

### Results and Discussion

When a DMSO solution of *p*-DNB was mixed with an aqueous DMSO solution of sodium hydroxide, the resulting reaction system showed absorption spectral changes shown in Figs. 1 and 2. All the absorption curves in Fig. 1 are corrected for the absorption of DMSO, since DMSO absorbs above 700 nm.<sup>1)</sup> The reaction system shows characteristic bands in the region

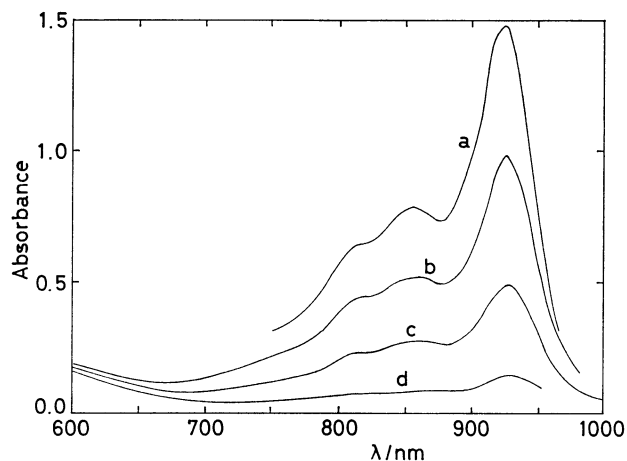


Fig. 1. Spectral change of the DMSO solution containing *p*-dinitrobenzene ( $3.34 \times 10^{-4}$  M), sodium hydroxide ( $1.00 \times 10^{-2}$  M), and 4% (v/v) water (25 °C). Starting time of scanning at 2.5 nm/s from longer wavelengths after mixing: a, 0.6 min; b, 2.4 min; c, 6 min; d, 11.4 min. Path length was 3.06 cm. All the curves are corrected for the absorption of DMSO.

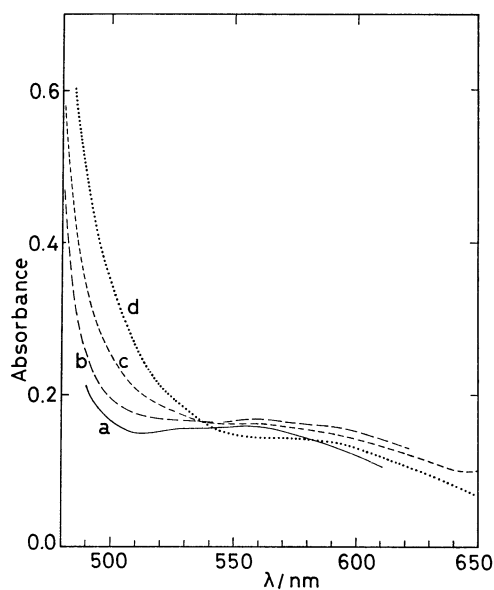


Fig. 2. Spectral change of the DMSO solution containing *p*-dinitrobenzene ( $3.42 \times 10^{-4}$  M), sodium hydroxide ( $9.5 \times 10^{-3}$  M), and 4% (v/v) water (25 °C). Starting time of scanning at 2.5 nm/s from longer wavelengths after mixing: a, 0.3 min; b, 1.3 min; c, 7.2 min; d, 60 min. Path length was 2.93 cm.

800–1000 nm and a weak band around 555 nm. The weak absorption shoulder is observed at *ca.* 580 nm in the final spectrum (curve d, Fig. 2). The shoulder is probably due to a small amount of a by-product. The bands in the region 800–1000 nm are similar to those of *p*-DNB<sup>•-</sup> in a rigid solution in 2-methyltetrahydrofuran at 77 K,<sup>4)</sup> and are assigned to *p*-DNB<sup>•-</sup>. The weak band around 555 nm is assumed to be the weak 475 nm band of *p*-DNB<sup>•-</sup> in the rigid solution.<sup>4)</sup> This was justified by calculating the absorption coefficient change at 560 nm. According to Shida and Iwata,<sup>4)</sup> *p*-DNB<sup>•-</sup> shows an intense band with vibrational structure in the range 380–430 nm. We were unsuccessful in scanning the spectral change in the range 400–500 nm when the reaction system was degassed, since an intense band rapidly developed at

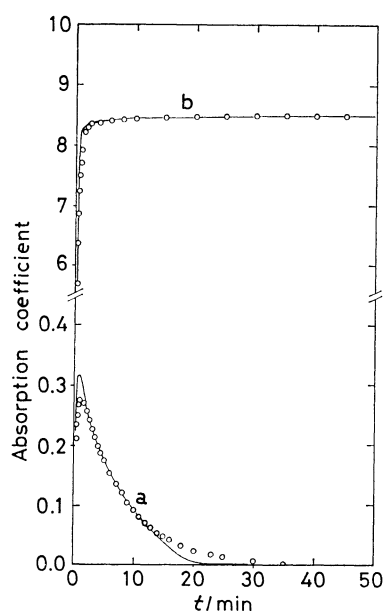


Fig. 3. Time courses (full lines) of absorption coefficient of the same solution as in Fig. 1 (25.0 °C). a, 930 nm; b, 430 nm. Circles show the values calculated according to Eqs. 1–4.

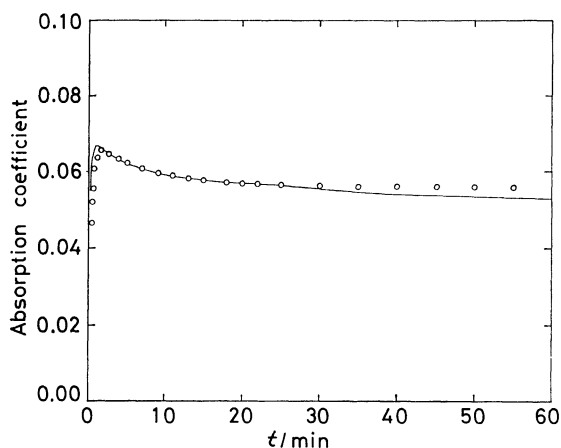


Fig. 4. Time course (full line) of 560-nm absorption coefficient of the same solution as in Fig. 1 (25.0 °C). Circles show the values calculated according to Eqs. 2 and 4.

430 nm. In the case of a similar reaction system open to the air, the initial band with a vibrational structure was observed at *ca.* 440 nm at 32 ms after mixing with a Hitachi rapid scan spectrophotometer RSP-2.<sup>3)</sup> The time dependence of absorption-coefficient at 930, 560, and 430 nm is shown in Figs. 3 and 4. Curve b in Fig. 3 indicates that the entire absorption at 430 nm is not due to one species, since the increase in the coefficient slows down at *ca.* 1 min after mixing. We thus infer that the band assigned to *p*-DNB<sup>•-</sup> initially appears in the range 400–500 nm.

The reaction system finally showed the 430 nm band identical with that of a similar solution of *p*-nitrophenol in the peak position and shape. A yellow substance was obtained by evaporating the solvent from the final reaction system under reduced pressure at *ca.* 60 °C. Treatment of the substance with aqueous hydrochloric acid gave *p*-nitrophenol. Thus, the final species showing the 430 nm band was identified as *p*-nitrophenoxide ion. The formation of *p*-nitrophenoxide ion in the reaction of *p*-DNB with hydroxide ion in aqueous DMSO open to the air has also been identified spectroscopically by Bowden and Cook.<sup>5)</sup> The yield of *p*-nitrophenoxide ion based on spectroscopic estimation was over 90%. Thin-layer chromatography also showed *p*-nitrophenol as the major product. The production of nitrite ion was confirmed by the brown ring test.

The formation of the labile *p*-DNB<sup>•-</sup> in the reaction system was confirmed by ESR spectroscopy. The generation of *p*-DNB<sup>•-</sup> in a similar reaction system has been reported by Bilkis and Shein.<sup>6)</sup> The reaction system under study showed a strong ESR signal. The hyperfine structure of the ESR spectrum (Fig. 5) is in line with that of the *p*-DNB<sup>•-</sup> having two equivalent nitrogen atoms. The splitting constants,  $a_N = 1.68$  and  $a_H = 1.12$  G, agree with the reference values.<sup>7)</sup> The time dependence of relative ESR-signal intensity of *p*-DNB<sup>•-</sup> in the reaction system at *ca.* 24 °C resembles that of the absorption coefficient change at 930 nm in Fig. 3. No other radical species was found in the ESR spectrum of the reaction system. The result eliminates all the schemes in which other free radicals produced reversibly should live together for a length of time with *p*-DNB<sup>•-</sup>, and which do not give the pseudo-first order decomposition of *p*-DNB<sup>•-</sup>, because the decomposition of *p*-DNB<sup>•-</sup> obeys the pseudo-first order kinetics.<sup>1)</sup> Thus *p*-DNB<sup>•-</sup> is not produced from a Meisenheimer-type complex.

The formation of *p*-DNB<sup>•-</sup> in DMSO is not due to the electron transfer from methylsulfinylmethanide<sup>8)</sup>

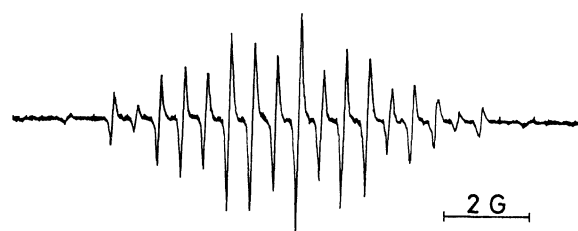


Fig. 5. ESR Spectrum of the same solution as in Fig. 1 (*ca.* 24 °C).

to *p*-DNB, since the mixture obtained by mixing an aqueous solution of sodium hydroxide with an *N,N*-dimethylformamide solution of *p*-DNB showed the same characteristic bands in the region 800–1000 nm as in Fig. 1.

The DMSO solution containing *p*-DNB ( $5.89 \times 10^{-4}$  M), *p*-nitrophenol ( $2.56 \times 10^{-3}$  M), sodium *p*-nitrophenoxide ( $1.25 \times 10^{-3}$  M), and 4% (v/v) water showed no characteristic band in the region above 600 nm. The formation of *p*-DNB<sup>•−</sup> is, therefore, not ascribed to electron transfer to *p*-DNB from the *p*-nitrophenol or *p*-nitrophenoxide ion produced by the conventional mechanism.

In a similar reaction system of *p*-DNB and hydroxide ion in aqueous DMSO solution, the production of the short-lived hydroxyl radical has been confirmed by Bilkis and Shein by means of spin-trapping with 2-nitroso-2-methylpropane.<sup>6)</sup>

Thus, the formation of *p*-DNB<sup>•−</sup> is probably due to the direct electron transfer from hydroxide ion to *p*-DNB. According to the electron transfer theory proposed by Nagakura and Tanaka,<sup>9,10)</sup> nucleophilic aromatic substitution should proceed *via* the anion radical resulting from the one-electron transfer from the highest occupied orbital of a nucleophilic reagent to the lowest vacant orbital of an aromatic molecule. The energy level of the highest occupied orbital should be higher than that of the lowest vacant orbital. The lowest-vacant energy level of *p*-DNB can be estimated to be  $-6.14$  eV from the values<sup>11)</sup> of the lowest  $\pi$ - $\pi^*$  transition energy (4.22 eV) and ionization potential (10.36 eV) of *p*-DNB. The energy level is sufficiently lower by 4.04 eV than the occupied energy level of OH<sup>−</sup> ( $-2.1$  eV<sup>9)</sup>). The energy level difference of 4.04 eV would not be small in the DMSO solution owing to the poor solubility of OH<sup>−</sup> in DMSO.<sup>12)</sup> *p*-DNB<sup>•−</sup> can be formed as a result of the direct electron transfer from hydroxide ion to *p*-DNB.

The plot of logarithmic absorption coefficient ( $\log a$ ) at 930 nm *vs.* time *t* is shown in Fig. 6. We see that the decomposition of *p*-DNB<sup>•−</sup> obeys the pseudo-first order kinetics from 2.5 min. The absorption coefficient

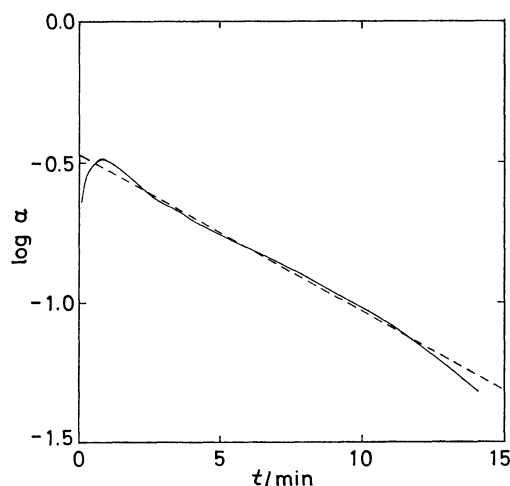


Fig. 6. Plot of logarithmic 930-nm absorption coefficient *vs.* time for curve a in Fig. 3.

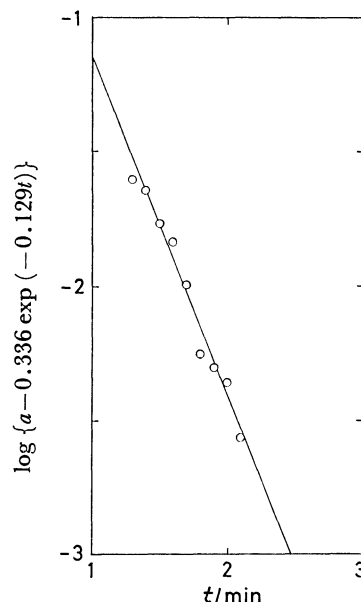


Fig. 7. Plot of  $\log\{a - 0.336 \times \exp(-0.129t)\}$  *vs.* time. Here the values of *a* are those of curve a in Fig. 3.

is expressed by  $0.336 \times \exp(-0.129t)$  from 2.5 min. From 0.5 min to 2.5 min the  $\log a$  values lie over a straight line, though all the  $\log a$  values lie on or below the corresponding line in the case of *o*-DNB.<sup>1)</sup> This indicates that at the initial stage the decomposition of *p*-DNB<sup>•−</sup> consists of two kinds of parallel reactions. One of the reactions is probably the same as that where *o*-DNB<sup>•−</sup> decomposes through the whole reaction course.<sup>1)</sup> The degree of the overlying of  $\log a$  (Fig. 6) varies to some extent in each measurement. Thus the other reaction, apparently observed at the initial stage, is very sensitive to the experimental conditions. As shown in Fig. 7, the plot of  $\log\{a - 0.336 \times \exp(-0.129t)\}$  *vs.* *t* is linear. This indicates that the reaction of *p*-DNB<sup>•−</sup> is of the pseudo-first order. The other may therefore be the rapid reaction of *p*-DNB<sup>•−</sup> with a slight amount of the unknown intermediate appearing in a steady state at the initial stage.

We denote the initial concentrations of *p*-DNB and sodium hydroxide by  $[p\text{-DNB}]_0$  and  $[\text{NaOH}]_0$ , respectively. Figure 8 shows that the decomposition of *p*-DNB<sup>•−</sup> is relatively fast and of the first order in the case of  $[\text{NaOH}]_0/[p\text{-DNB}]_0 \geq 3$ , and that the decomposition is extremely slow in the case of  $[\text{NaOH}]_0/[p\text{-DNB}]_0 < 3$ . The slow decomposition is not due to the irradiation of the 930 nm light, since the decomposition proceeded in the absence of the light. It is indicated that the fast decomposition of *p*-DNB<sup>•−</sup> requires hydroxide ion, and that the conditions of  $[\text{NaOH}]_0 \geq 3[p\text{-DNB}]_0$  are necessary for the production of *p*-nitrophenoxide ion. Thus, the present reaction does not proceed by the  $S_{\text{RN}}1$  mechanism,<sup>13,14)</sup> which is characterized by the unimolecular decomposition of the anion radical. The hydroxide ion equivalent to  $[p\text{-DNB}]_0$  will be consumed for ionizing *p*-nitrophenol, because *p*-nitrophenol scarcely dissociates in the DMSO solution containing 4% (v/v) water in the absence of sodium hydroxide.

Thus, in analogy with the case of *o*-DNB,<sup>1)</sup> the two

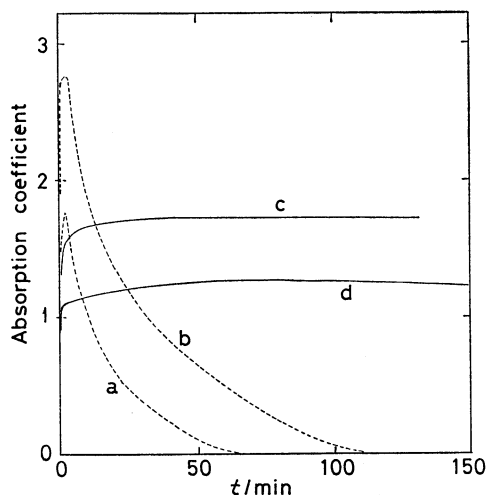
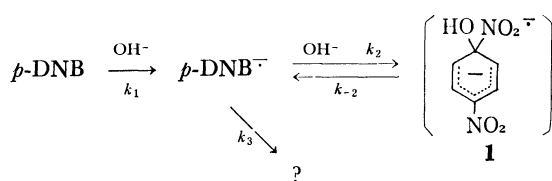


Fig. 8. Time courses of 930-nm absorption coefficient of the following DMSO solution containing 4% (v/v) water (25.0 °C).

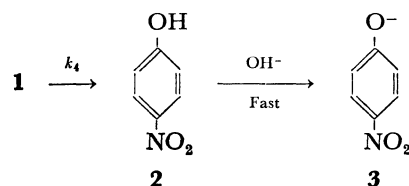
	$[p\text{-DNB}]_0$ $\times 10^3, \text{ M}$	$[\text{NaOH}]_0$ $\times 10^2, \text{ M}$	$[\text{NaOH}]_0/[p\text{-DNB}]_0$
a	2.47	1.00	4.05
b	3.34	1.00	2.99
c	3.36	0.69	2.1
d	3.34	0.33	1.0

possible schemes for the present reaction may be written as shown in Scheme 1 where  $k_i$  denotes the rate constant for the  $i$ th step, and both  $k_1$  and  $k_2$  contain  $[\text{NaOH}]_0$ . Of course,  $k_3$  is of the pseudo-first order and is negligible after 2.5 min. Since no band of intermediates other than that of  $p\text{-DNB}^-$  is found in Figs. 1 and 2, we make the steady state treatment for the concentrations of **1** and **4**.

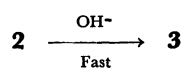
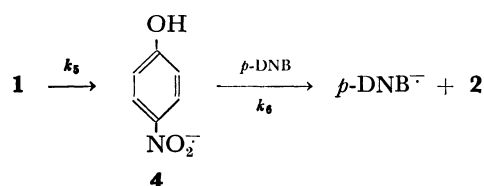
According to Scheme 1(a), the absorption coefficient



(a)



(b)



Scheme 1.

changes at 930 and 430 nm with time are expressed below under the conditions of  $[p\text{-DNB}]_0 \ll [\text{NaOH}]_0$ .

$t < 2.5 \text{ min}$ :

$$a(930 \text{ nm}) = \frac{k_1 \epsilon_R [p\text{-DNB}]_0}{k_1 - k_2' - k_3} \times [\exp\{-(k_2' + k_3)t\} - \exp(-k_1 t)] \quad (1)$$

$$a(430 \text{ nm}) = \frac{k_2' \epsilon_3 [p\text{-DNB}]_0}{k_2' + k_3} - \frac{k_1 [p\text{-DNB}]_0}{k_1 - k_2' - k_3} \times \left( \frac{k_2' \epsilon_3}{k_2' + k_3} - \epsilon_R' \right) \exp\{-(k_2' + k_3)t\} - \frac{[p\text{-DNB}]_0}{k_1 - k_2' - k_3} \times (k_1 \epsilon_R' - k_3 \epsilon_3) \times \exp(-k_1 t) \quad (2)$$

$t \geq 2.5 \text{ min}$ :

$$a(930 \text{ nm}) = \frac{k_1 \epsilon_R [p\text{-DNB}]_0}{k_1 - k_2'} \times \exp(-k_2' t) \quad (3)$$

$$a(430 \text{ nm}) = \epsilon_3 [p\text{-DNB}]_0 - \frac{k_1 [p\text{-DNB}]_0}{k_1 - k_2'} \times (\epsilon_3 - \epsilon_R') \times \exp(-k_2' t) \quad (4)$$

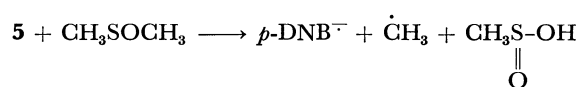
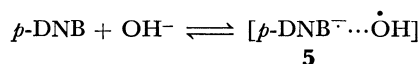
Here  $k_2' = k_2 k_4 / (k_{-2} + k_4)$ , and  $\epsilon_R$  and  $\epsilon_3$  are molar absorption coefficients of  $p\text{-DNB}^-$  and **3**, respectively. Equations 3 and 4 are similar to the corresponding equations for the case of *o*-DNB,<sup>1)</sup> in which the terms including  $\exp(-k_1 t)$  are neglected. The values calculated according to Eqs. 1–4 are plotted in Fig. 3 by assuming the following values;  $k_1 = 2.88 \text{ min}^{-1}$ ,  $k_2' = 0.129 \text{ min}^{-1}$ ,  $k_3 = 0.002 \text{ min}^{-1}$ ,  $\epsilon_R(930 \text{ nm}) = 9.61 \times 10^2$ ,  $\epsilon_R'(430 \text{ nm}) = 2.49 \times 10^4$ , and  $\epsilon_3(430 \text{ nm}) = 2.54 \times 10^4$ . As compared with the corresponding rate constants of  $k_1 = 0.638 \text{ min}^{-1}$  and  $k_2' = 0.0519 \text{ min}^{-1}$  for the case of *o*-DNB,<sup>1)</sup>  $p\text{-DNB}^-$  has formation and decomposition rates greater than those of *o*-DNB<sup>−</sup>.

Equations 2 and 4 can be applied to the absorption coefficient change at 560 nm. The result obtained by assuming  $\epsilon_R''(560 \text{ nm}) = 205$  and  $\epsilon_3'(560 \text{ nm}) = 168$  is shown in Fig. 4. Figures 3 and 4 show that the calculated values of absorption coefficients at 930, 560, and 430 nm fairly agree with those observed. The value of  $\epsilon_R'(430 \text{ nm})$  is considerably larger than that (*ca.*  $1.6 \times 10^4$ ) of the 420 nm band of  $p\text{-DNB}^-$  in the rigid solution at 77 K.<sup>4)</sup> The value of  $\epsilon_3(430 \text{ nm})$  is smaller than that of  $3.17 \times 10^4$  for *p*-nitrophenoxide ion in a similar solution. This difference seems to be due mainly to the initial rapid reaction of  $p\text{-DNB}^-$ . The value of  $3.34 \times 10^{-4} \text{ M}$  is calculated for the maximum concentration of  $p\text{-DNB}^-$  by dividing the observed maximum absorption coefficient (0.321) at 930 nm (Fig. 3) by  $\epsilon_R(930 \text{ nm}) = 9.61 \times 10^2$ . The calculation shows that  $p\text{-DNB}$  was almost converted into  $p\text{-DNB}^-$  within 0.7 min. The anion radical is, therefore, probably formed in the main reaction path.

The relation of  $k_1 = 22.3 k_2'$  and  $k_2' = 64.5 k_3$  is obtained from the values assumed above for the case of Scheme 1(a). Under the conditions  $k_1 \gg k_2' \gg k_3$ , Scheme 1(b) gives approximate expressions similar to those to which Eqs. 1–4 can be reduced. Accordingly, Scheme 1(b) is also possible in addition to Scheme 1(a). The mechanisms including the reaction to re-

produce *p*-DNB instead of the reaction step denoted by  $k_3$  in Scheme 1 are also considered. Under the conditions  $k_1 \gg k_2' \gg k_3$ , however, the mechanisms give approximate expressions which cannot explain the appearance of the initial overlying of  $\log a$  and are probably impossible. In conclusion, the kinetic results strongly suggest that *p*-DNB<sup>-</sup> is the precursor in the reaction, though we do not know which to select, Scheme 1 (a) or (b).

From the studies on the photosubstitution of 3,5-dinitroanisole<sup>15,16)</sup> and on the reaction between DMSO and hydroxyl radical<sup>17)</sup> the generation of *p*-DNB<sup>-</sup> may be accounted for by the following mechanism as in the case of *o*-DNB<sup>-</sup>:<sup>1)</sup>



The reaction between **5** and DMSO may be extremely rapid, because the rate constant for the reaction of hydroxyl radical with DMSO in aqueous solution is  $5 \times 10^9 \text{ M}^{-1} \text{ s}^{-1}$  at 25 °C.<sup>17)</sup> The methyl radical would undergo a rapid reaction. Thus, only *p*-DNB<sup>•−</sup> may survive in the present reaction system. The production of short-lived hydroxyl radical<sup>6)</sup> supports the formation of **5**.

## References

- 1) T. Abe and Y. Ikegami, *Bull. Chem. Soc. Jpn.*, **49**, 3227 (1976).
- 2) All the references suggesting anion-radical precursors in the nucleophilic aromatic substitution were cited in Ref. 1.
- 3) T. Abe, *Chem. Lett.*, **1973**, 1339.
- 4) T. Shida and S. Iwata, *J. Phys. Chem.*, **75**, 2591 (1971).
- 5) K. Bowden and R. S. Cook, *J. Chem. Soc., B*, **1971**, 1765.
- 6) I. I. Bilkis and S. M. Shein, *Tetrahedron*, **31**, 969 (1975).
- 7) P. H. Rieger and G. K. Fraenkel, *J. Chem. Phys.*, **39**, 609 (1963).
- 8) G. A. Russell, E. G. Janzen, and E. T. Strom, *J. Am. Chem. Soc.*, **86**, 1807 (1964).
- 9) S. Nagakura and J. Tanaka, *Bull. Chem. Soc. Jpn.*, **32**, 734 (1959).
- 10) S. Nagakura, *Tetrahedron*, **19**, Suppl. 2, 361 (1963).
- 11) M. D. Gordon and J. F. Neumer, *J. Phys. Chem.*, **78**, 1868 (1974).
- 12) A. J. Parker, *Quart. Rev.*, **16**, 163 (1962).
- 13) J. K. Kim and J. F. Bunnett, *J. Am. Chem. Soc.*, **92**, 7463, 7464 (1970).
- 14) J. F. Bunnett, *Acc. Chem. Res.*, **5**, 139 (1972).
- 15) G. P. de Gunst and E. Havinga, *Tetrahedron*, **29**, 2167 (1973).
- 16) W. G. Dauben, L. Salem, and N. J. Turro, *Acc. Chem. Res.*, **8**, 41 (1975).
- 17) B. C. Gilbert, R. O. C. Norman, and R. C. Sealy, *J. Chem. Soc., Perkin Trans. 2*, **1975**, 303.